Available online at www.sciencedirect.com

ScienceDirect

Physics Procedia 12 (2011) 345–352

Physics Procedia

Laser Cladding of Vanadium-Carbide Tool Steels for Die Repair

J. Leunda, C. Soriano*, C. Sanz, V. García Navas

Tekniker-IK4, Advance Manufacturing Technologies Unit, Avda. Otaola 20, 20600 - Eibar (Gipuzkoa), Spain

Abstract

A study of the laser cladding of powder metallurgical tool steels has been carried out. CPM 10V and Vanadis 4 Extra tool steel powders have been deposited on Vanadis 4 Extra tool steel plates, for repairing purposes, using a Nd:YAG laser. The microstructure of the laser cladding samples was investigated using optical and scanning electron microscopes. The volumetric fraction of retained austenite was evaluated by X-ray diffraction and microhardness profiles were measured. Crack free 700 HV 0.3 cladding tracks were achieved with both materials and coatings show a microstructure of carbides embedded in a martensite plus retained austenite matrix.

Keywords: powder metallurgy; tool steels; laser cladding; Nd:YAG laser

1. Introduction

Cold and hot shaping industry is nowadays subject to new challenges in the tool manufacturing and repair field as consequence of the requirements generated by the introduction of new forming materials (mainly in the automotive sector, like the High Strength Steels - HSS) to guaranty the most increasing safety exigencies under driving conditions. Unfortunately, HSS are extremely aggressive for tools and dies and force the die sector to use new working tool materials for cutting, deep-drawing and bending dies.

New powder metallurgical tool steels, with an excellent combination of toughness, hardness and wear resistance, are appearing to overcome current deficiencies. These tool steels, usually vanadium carbide steels, are used to shape HSS, all of which combine high yield strength with high elongation and considerable work hardening.

Some processes used with the traditional tools steels cannot be used any longer with these new materials. As an example, machining failures or tool damage in service are conventionally repaired by tungsten inert gas (TIG), gas metal arc welding (GMAW) or high velocity oxygen fuel (HVOF) techniques, which turn to be unfeasible processes with these materials mainly based on powder metallurgical steels.

In this frame, the laser cladding technique arises as a good alternative that offers a good metallurgical bonding

* Corresponding author. Tel.: +34-943-206-744; Fax: +34-943-202-744.
E-mail address: csoriano@tekniker.es.

doi:10.1016/j.phpro.2011.03.044

with the substrate offering deposits of coating material with wear, corrosion and high-temperature oxidation resistance that guarantees the toughness of the base material [1]. Some research studies can be found in the state of the art concerning the laser cladding of powder metallurgical steels to produce hard-facing materials on low alloy and carbon steels. For instance, Hu *et al.* deposited CPM 9V and 10V materials on AISI 1045 steel plates or rollers via laser cladding [2]. Another study assesses the abrasive wear behavior of CPM 10V, CPM15V, CPM 9V and AISI M4 deposited by laser cladding on carbon steel substrates compared to a reference material AISI D2 tool steel [3]. This group of high vanadium-containing tools steels above mentioned has proven to be successful in achieving excellent wear resistance [4]. However, few publications study the deposition of those powder metallurgical tool steels on hardened substrates. The aim of this paper is to study the laser cladding process of such materials when deposited on heat treated Vanadis 4 Extra, hereafter called Vanadis 4, tool steel with the objective to face future repair tasks.

2. Experimental

Heat treated Vanadis 4 (61-63 HRC) plates of 150x80x20 mm were used as the substrates, and CPM 10V and Vanadis 4 alloy powders as the coating materials. The substrate surfaces were machined before the laser treatment trying to simulate a real tool situation. The chemical composition of the substrate and the clad materials, obtained by chemical analysis, are listed in Table 1. Deposition materials were gas atomized obtaining spherical powders, as can be observed in Figure 1, with a grain size between 45-90 μm.

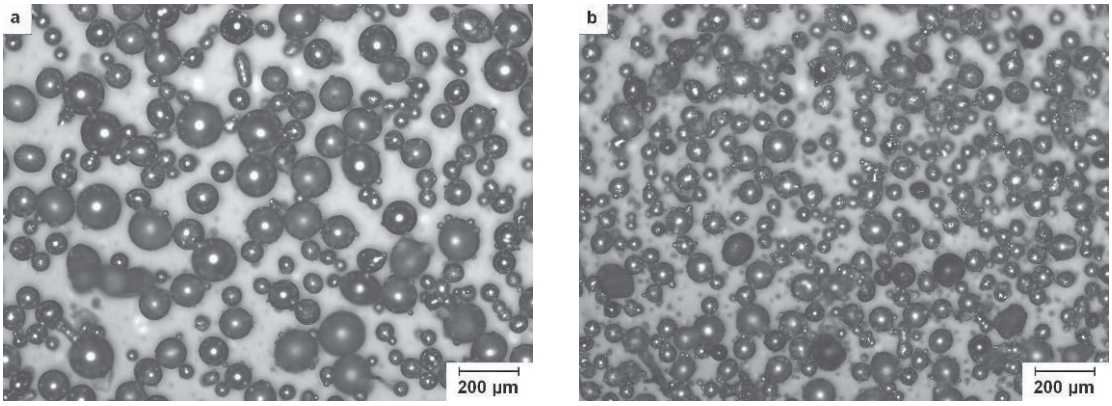

Figure 1. CPM 10V (a) and Vanadis 4 (b) powders

Table 1. Chemical composition (wt. %) of the studied materials

Material	C	Cr	Mn	Mo	P	S	Si	V
Vanadis 4 Extra	1.40	4.70	0.40	3.50	-	-	0.40	3.70
CPM 10V	2.43	5.25	0.49	1.29	0.01	0.07	0.91	9.64

The laser cladding was conducted using a 2.2 kW diode pumped continuous wave Nd:YAG laser. The laser beam was guided to the working area by a 0.6 mm diameter circular fiber connected to a laser head with an optical system, able to provide a defocused 2.7 mm circular spot with a Gaussian irradiance profile at the selected working distance. A powder injection system was used to deliver alloy powders into the melt pool through a discrete laser cladding nozzle. Argon was used as the carrier gas and Helium as the coaxial shielding gas, to prevent surface oxidation. The substrate was preheated to a temperature below its maximum tempering temperature in order to prevent cracking of the coating or the substrate. Single layer multi-track coatings with desired overlap ratio were carried out obtaining 0.6 mm thick layers, covering an area of 60x15 mm. The most relevant processing parameters are summarized in Table 2.

Table 2. Parameters for laser cladding

Laser power (KW)	0.9, 1.2
Scanning speed (mm/s)	15
Powder flow rate (g/min)	5, 10, 15
Gas pressure (bar)	2
Overlap (%)	35

Microstructural and hardness analyses were carried out by optical and scanning electron microscopy (SEM) and by microhardness testing on transverse sections respectively. The samples were polished with diamond powder and chemically etched in a solution of HNO_3:HCl:H_2O with the volumetric proportion of 1:2:3. Microhardness measurements were carried out, using a microhardness tester, in the centre of the fifth track, from the surface to the core (vertical) and across the clad zone, parallel to the original surface at 0.2 mm above it (horizontal). An X-ray diffractometer with parallel beam (2 mm diameter pinhole) and Cr radiation, operated at 40 kV and 40 mA was used to obtain diffractograms of the two coatings. The measurements were done at the centre of the surface of each coating. Due to the low penetration of X-rays, the information obtained comes from the very surface, around 5-10 μm deep. The diffractograms obtained allow comparing qualitatively the retained austenite fraction in each coating.

3. Results and Discussion

3.1. Effect of the process parameters

Laser power and the scanning speed are the most relevant parameters concerning the heat input, apart from the spot size, which has been fixed. The powder flow rate is also important due to the laser beam attenuation effect that strongly depends on the powder amount between the laser source and the base metal. The laser cladding process parameters were carefully chosen, in order to prevent or avoid cracking of the substrate. High alloy tool steels tend to crack very easily due to the tensile residual stresses generated in the base metal, all around the coating. Therefore thermal distortions should be minimized reducing the heat input over the substrate.

Similar results were obtained with both coating materials, as it was expected because of their resemblance to each other. Defect free coatings could only be generated with the lowest powder feeding rate, i.e. with 5 g/min (Figure 2(a) and Figure 2(c)). When increasing this parameter, higher tracks with low aspect ratio (width/height) were produced, thus making it difficult for the alloy powder to access the edge between the preceding track and the substrate. This entails a linear lack of union in those zones, as it can be observed in Figure 2(b) and Figure 2(d), making them potential crack initiation sites.

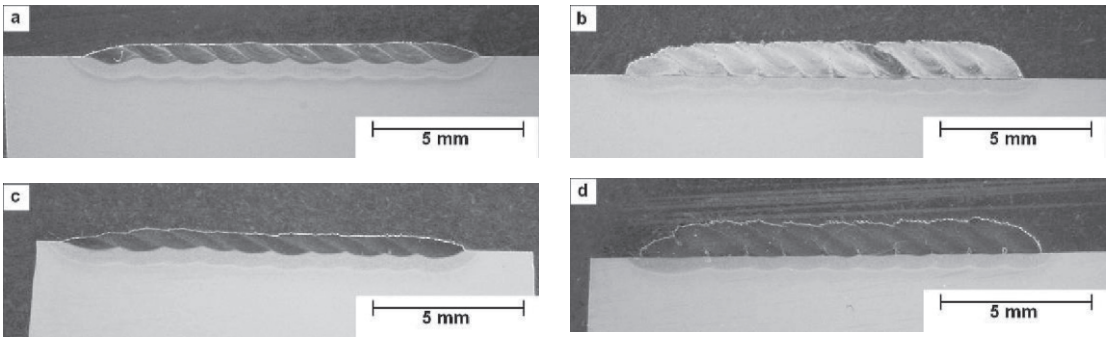

Figure 2. Optical macrographs showing CPM 10V (a- 1.2 KW and 5 g/min, b- 1.2KW and 15 g/min) and Vanadis 4 (c- 1.2 KW and 5 g/min, d- 1.2KW and 15 g/min) coatings

Concerning power, coatings produced with 1.2 KW were higher than those obtained with 0.9 KW. The amount of molten powder increases with higher laser power, reducing consequently the waste material and improving the process efficiency. Hence, the coatings chosen for further study were the ones generated with a laser power of 1.2 KW and a powder flow rate of 5 g/min.

3.2. Microstructure

Three clearly distinguishable regions are observed in the cladding tracks with both powder alloys as shown in Figure 3: clad zone (CZ), interface zone (IZ) and the heat-affected zone (HAZ). Nevertheless, the two latter ones are produced by purely thermal effects being, therefore, similar in both coatings. In the HAZ, the martensite of the substrate material has been re-tempered, being more bainite-like in the upper region due to the higher temperatures achieved in this area. Substrate carbides have been affected neither in size nor in number. In the IZ, temperatures above the critical austenization value have been achieved, followed by a rapid quenching process resulting in a quenched martensite and retained austenite matrix, with a major content of austenite in the upper region. Carbides have been partially dissolved in this region due to the high temperatures achieved, resulting in a noticeable reduction of their number in comparison with the unaffected material, as it can be seen in Figure 4.

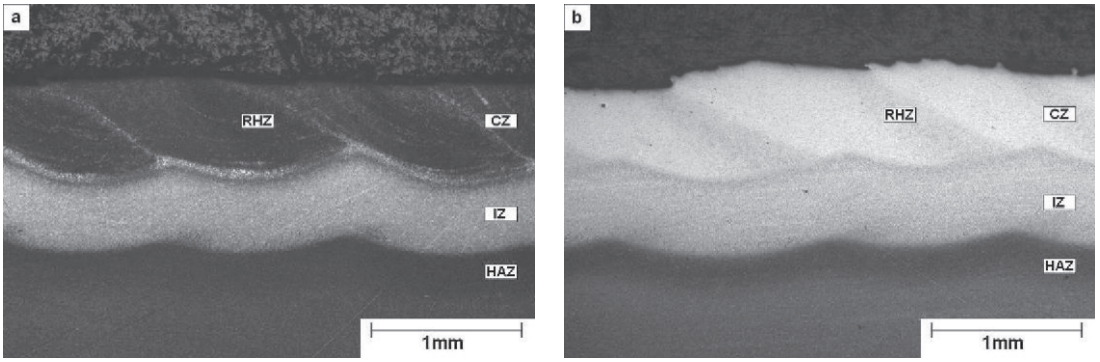

Figure 3. Optical macrographs showing the different zones of CPM 10V (a) and Vanadis 4 (b) coatings (CZ: Clad zone, IZ: Interface zone, HAZ: Heat affected zone, RHZ: Re-heated zone)

Regarding the CPM 10V coating, a white narrow layer is observed between the CZ and the IZ. Carbides in this layer have been almost completely dissolved due to the high temperatures achieved (close to the melting point). Moreover, being the carbon content of the CPM 10V higher than that of the Vanadis 4, carbon migration may take place from the coating to the base material, increasing the carbon content of the metal matrix. The combination of those two effects promotes the retained austenite formation to the detriment to carbide precipitation, thus resulting in a soft, mainly austenitic and almost carbide free layer. A different result is obtained in the case of Vanadis 4, since the alloy powder and the base material are compositionally equal, no carbon migration occurs, enabling the primary carbide precipitation within a mainly austenitic matrix.

Each cladding track is re-heated during the deposition of the subsequent track. This results in a tempered or re-heated zone (RHZ) in which the microstructure has changed (dark bands in Figure 4(a) and Figure 4(b)). Out of those regions, the CZ of the CPM 10V coating shows a quenched martensite and retained austenite matrix with rod-like vanadium and chromium rich carbides in the grain boundaries and tiny rod-like and globular carbides in the center of the cellular structure (Figure 5(a)). In contrast, in the RHZ, where a tempering process has taken place, the quenched martensite and part of the retained austenite have been transformed into tempered martensite. With regard to the carbides, the fine carbides of the center of the track have gathered forming bigger globular carbides uniformly scattered within the matrix (Figure 5(b)).

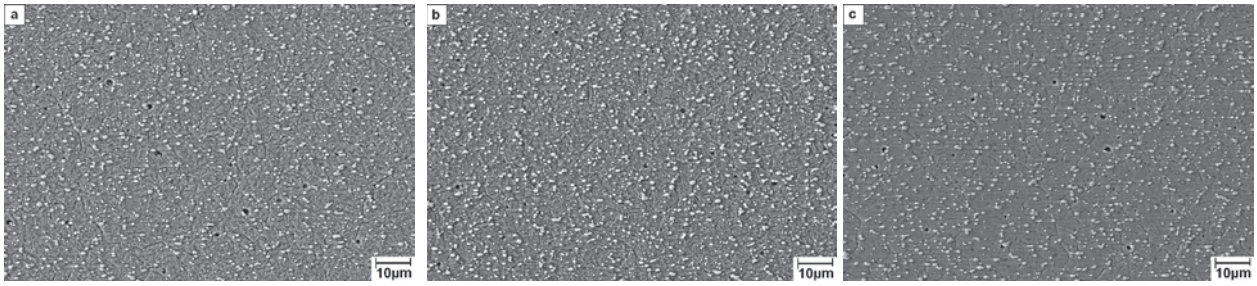

Figure 4. SEM micrographs showing the base metal (a), HAZ (b) and IZ (c) carbide distributions of the Vanadis 4 coating

The Vanadis 4 coating shows a cellular structure with vanadium and molybdenum rich carbides located almost exclusively along the grain boundaries. The metal matrix is again formed by a mixture of quenched martensite and retained austenite (Figure 5(c)). The carbide size and distribution remains unchanged in the RHZ of the Vanadis 4 coating, while the quenched martensite and part of the retained austenite of the matrix have transformed into tempered martensite (Figure 5(d)).

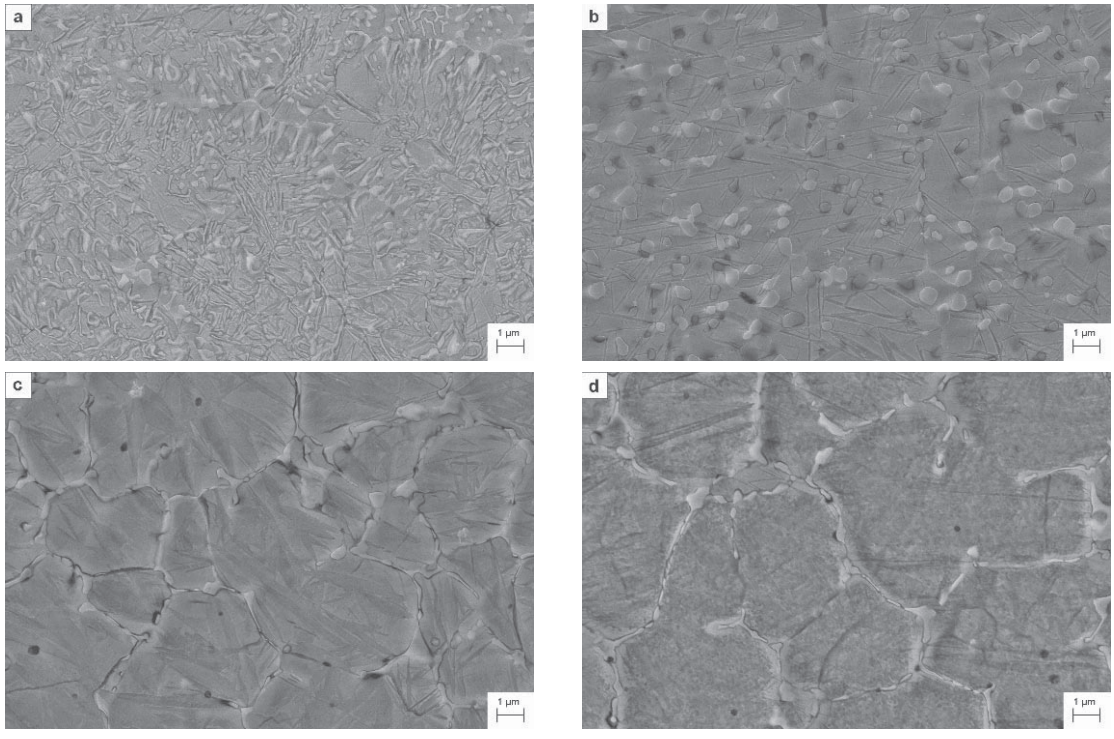

Figure 5. SEM microghraphs showing the representative microstructures of CPM 10V (*a*- in the center of the track and *b*- in the RHZ) and Vanadis 4 (c- in the center of the track and *d*- in the RHZ) coatings

The coatings are free of cracks, according to visual examination of the surface and cross sectional view using optical microscope and SEM. Both materials show similar porosities. Some sporadic pores of 10 – 40 µm are found in the coatings presumably due to the gas inclusions which are highly dependent of the solidification geometry. Tiny (less than 1 µm, as shown in Figure 5) uniformly distributed pores are also found all over the coatings, which are the result of the degassing as the clad solidifies [5].

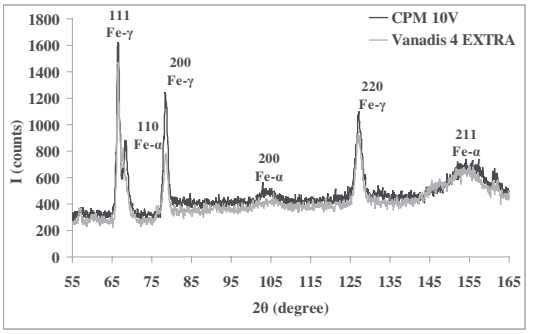

Figure 6. X-ray diffraction scans of CPM 10V and Vanadis 4 coatings, obtained using Cr radiation

3.3. Microhardness

Figure 6 plots the X-ray diffraction scans of the CPM 10V and Vanadis 4 coatings, using Cr radiation. The Fe-γ peaks indicate the presence of certain fraction of retained austenite being in agreement with the microstructure results found in the CZ of both coatings. Particularly the CPM 10V (200) Fe-γ diffraction peak is slightly higher than that of the Vanadis 4, indicating that the latter presents a slightly lower volume fraction of austenite, and therefore a more martensitic matrix with higher expected hardness. In contrast, the lower carbide content of this coating affects the overall hardness of the clad in the opposite way. The combined effect of the volumetric austenite fraction and the carbide content on the microhardness is shown in Figure 7. Microhardness values of about 700 HV 0.3 are achieved in both cladding tracks, being slightly lower than the substrate hardness, mainly due to the retained austenite of the coatings. Below the CZ, both microhardness profiles look exactly the same, except for the lower value measured at 0.6 mm below the surface in the case of the CPM 10V coating, related to the soft, mainly austenitic thin layer previously discussed.

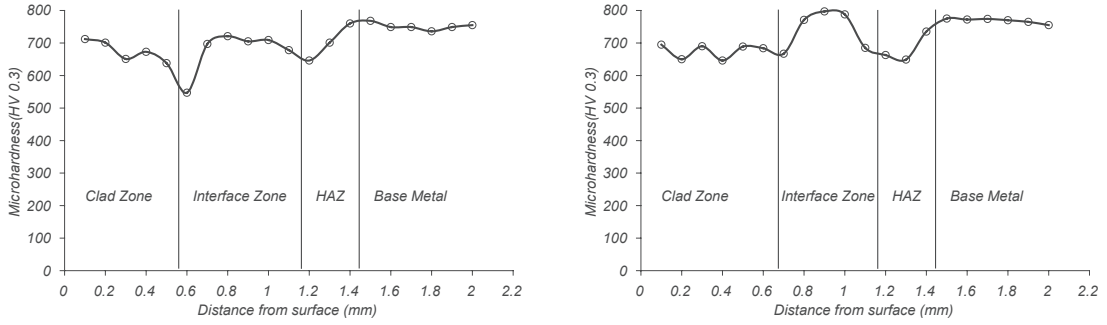

Figure 7. Microhardness profiles of CPM 10V (left) and Vanadis 4 (right) coatings measured from the surface to the core of the coated plate

Figure 8 shows the horizontal microhardness profiles measured in the CZ of both coatings at 0.2 mm above the original surface. The CPM 10V coating presents higher overall hardness, but a more heterogeneous profile due to the microstructure differences between the area of the tracks, unaffected by the subsequent depositions, and the RHZ. In the unaffected track centers tiny multi-shape carbides are scattered all over the metal matrix, leaving little space between them, while in the RHZ larger globular carbides are distributed with major carbide free regions, so the probability of the indentations to hit a carbide is much lower in the RHZ than in the track center, resulting in a lower hardness values in that region. With regard to the Vanadis 4 coating, the only difference between those two areas is related to the tempering of the matrix being the carbide shape and distribution similar in both zones. The hardness profile is therefore smoother, as is the microstructure variation.

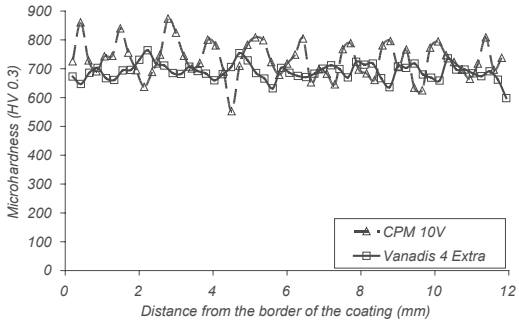

Figure 8. Horizontal microhardness profiles of CPM 10V and Vanadis 4 coatings measured at 0.2 mm above the original surface

The hardness of the coatings can be further increased by a post heat-treatment [3]. The correct selection of the proper heat-treatment is critical, though; too high tempering temperatures could be detrimental to the substrate hardness. In our case, a double tempering process could be the ideal choice, considering that both the substrate and the coating materials are highly alloyed tool steels in which secondary hardening occurs as a result of the transformation of the retained austenite to martensite and the precipitation of secondary alloy carbides on cooling from the tempering temperature [6].

4. Summary and conclusions

Coatings of CPM 10V and Vanadis 4 produced by laser cladding have been studied. Similar hardness values have been obtained with both coatings, although slight differences were observed in the microstructures.

Three different zones are observed in the transverse sections of both coatings: Clad zone (CZ), interface zone (IZ) and heat affected zone (HAZ).

The structure of the HAZ is formed of unaltered substrate carbides embedded in a tempered martensite matrix, being similar in both coatings. The IZ shows a quenched martensite and retained austenite matrix with less carbides than in the substrate or in the HAZ. A thin layer is observed in both coatings between the IZ and the CZ. This layer is mainly austenitic in both coatings, being almost carbide free in the CPM 10V coating, while in the Vanadis 4 coating a significant amount of carbides is found.

In the CZ of the CPM 10V coating rod-like and globular carbides are scattered all around the martensite and retained austenite matrix. Carbides are gathered in the RHZ to become bigger and globular, while the metal matrix is tempered. The Vanadis 4 CZ shows a cellular structure with carbides located along the grain boundaries. Neither the carbide distribution nor the amount is altered in the RHZ, although the austenite and the martensite of the matrix are tempered.

A hardness of roughly 700 HV 0.3 is measured in both coatings, being more heterogeneous in the case of the CPM 10V, due to the variation of the carbide distribution in the RHZ.

These results demonstrate that the microstructure obtained on the coatings applied directly by laser cladding technique is similar to that of a quenched high alloy tool steel and results to be suitable for repairing this kind of tools. Future further treatments are being studied to improve hardness and microstructure.

Acknowledgements

The authors thank to the MANUNET program to have supported CLADIES project where this investigation has taken place and to the Basque Country Government (Industry, Commerce and Tourist Department) for the financial help received under the GAITEK program. Furthermore, we extend the acknowledgements to the Italian and Basque consortium of the project and especially to TROMESA for its close collaboration in this work.

References

[1] E. Toyserkani; A. Khajepour; S. Corbin: Laser cladding. CRC Press, 2005
[2] Y. P. Hu; C. W. Chen; K. Mukherjee: Development of a new laser cladding process for manufacturing cutting and stamping dies. In: Journal of materials science 33 (1998), 1287-1292
[3] S. H. Wang; J. Y. Chen; L. Xue: A study of the abrasive wear behaviour of laser-clad tool steel coatings. In: Surface & Coatings Technology 200 (2006), 3446-3458
[4] W. Stasko; K. E. Pinnow; R. B. Dixon: Proceeding of the 5th International Conference on Advanced Particulates materials and Process, Metal Powder Industries federation, Princeton, NJ,1997, p.401
[5] J. C. Ion: Laser processing of engineering materials. Elsevier Butterworth-Heinemann, 2005
[6] G. E. Totten: Steel heat treatment handbook. Taylor & Francis Group, 2006